Hindawi Publishing Corporation
International Journal of Photoenergy
Volume 2012, Article ID 569716, 10 pages
doi:10.1155/2012/569716

Research Article

Enhanced Visible Light Photocatalytic Activity of V_2O_5 Cluster Modified N-Doped TiO_2 for Degradation of Toluene in Air

Fan Dong, Yanjuan Sun, and Min Fu

College of Environmental and Biological Engineering, Key Laboratory of Catalysis Science and Technology of Chongqing Education Commission, Chongqing Technology and Business University, Chongqing 400067, China

Correspondence should be addressed to Fan Dong, dfctbu@126.com

Received 2 January 2012; Revised 19 February 2012; Accepted 20 February 2012

Academic Editor: Xuxu Wang

V_2O_5 cluster-modified N-doped TiO_2 (N-TiO_2/V_2O_5) nanocomposites photocatalyst was prepared by a facile impregnation-calcination method. The effects of V_2O_5 cluster loading content on visible light photocatalytic activity of the as-prepared samples were investigated for degradation of toluene in air. The results showed that the visible light activity of N-doped TiO_2 was significantly enhanced by loading V_2O_5 clusters. The optimal V_2O_5 loading content was found to be 0.5 wt.%, reaching a removal ratio of 52.4% and a rate constant of 0.027 min^{-1}, far exceeding that of unmodified N-doped TiO_2. The enhanced activity is due to the deposition of V_2O_5 clusters on the surface of N-doped TiO_2. The conduction band (CB) potential of V_2O_5 (0.48 eV) is lower than the CB level of N-doped TiO_2 (−0.19 V), which favors the photogenerated electron transfer from CB of N-doped TiO_2 to V_2O_5 clusters. This function of V_2O_5 clusters helps promote the transfer and separation of photogenerated electrons and holes. The present work not only displays a feasible route for the utilization of low cost V_2O_5 clusters as a substitute for noble metals in enhancing the photocatalysis but also demonstrates a facile method for preparation of highly active composite photocatalyst for large-scale applications.

1. Introduction

Environmental pollution and energy crisis are the two major global challenges faced by human beings. Semiconductor photocatalysis is green technology that allows the use of sunlight for the destruction of pollutants and conversion of solar energy to hydrogen, thus providing an attractive route to potentially solve the both problems [1–3]. The widely used photocatalyst TiO_2 is, however, only UV active due to its relatively large band gap [4, 5]. As UV light accounts for a small fraction (4%) of the sun's energy compared to visible light with a large fraction of 45%, the shift in the optical absorption of TiO_2 from the UV to the visible region is of significance for practical application of photocatalyst [6–8].

Visible light driven photocatalysis is one of the hottest topics worldwide [9–22]. Pioneered by Asahi et al. who reported that nitrogen doping can extend the optical absorption of TiO_2 into visible region and enhance the photocatalytic activity under visible light irradiation [9], many efforts have been devoted afterwards to developing nonmetal doped TiO_2 exhibiting enhanced visible light activities [10–14]. Among the various types of nonmetal doped TiO_2, N-doped TiO_2 is the most typical and has been intensively investigated for solar energy conversion and pollutants degradation [15–18]. However, nitrogen doping intrinsically favored the formation of defects that act as recombination center, which largely limited the photoactivity of N-doped TiO_2 under visible light illumination [19–22].

In order to improve the visible light photocatalytic performance of N-doped TiO_2, further modification has been employed, including codoping with nonmetals (C, S, F) [23–25], co-doping with metal ions (Fe, La, V) [26–28], noble metal deposition (Pt, Au) [29, 30] and metal oxide coupling (WO_3, PdO, ZrO_2) [31–33]. The modifications usually show promotive effects on visible light photocatalytic activity of N-doped TiO_2. The activity promotion is related to phase structure, optical absorption, charge transfer, and surface properties. Recently, nanoscale clusters have been utilized to modify different types of photocatalysts [34–42]. Highly enhanced photocatalytic activities over the investigated

cluster/photocatalyst composites systems, including $Ni(OH)_2/TiO_2$, $Cu(OH)_2/TiO_2$, CuO/self-doped TiO_2, V_2O_5/C-doped TiO_2, V_2O_5/TiO_2, vanadium species/N-doped TiO_2, Fe_2O_3/WO_3, and CdS/graphene have been observed [34–42]. However, to our knowledge, there are few reports on the enhanced photocatalytic activity over V_2O_5 cluster-modified N-doped TiO_2 up to now.

In our previous study, N-doped TiO_2 (N-TiO_2) photocatalyst was prepared by partial oxidation of TiN in air [43]. In the present study, we report the facile preparation of V_2O_5 cluster-modified N-doped TiO_2 nanocomposite for the first time through an impregnation-calcination method and enhanced visible light photocatalytic activity for degradation of toluene in air. The microstructure, optical, and surface properties of the resulted nanocomposites photocatalysts were investigated systematically by XRD, Raman, TEM, XPS, UV-vis DRS, and PL. Based on the characterization results, a new mechanism on the promotive effects of V_2O_5 cluster modification on the charge transfer and visible light photocatalysis of N-doped TiO_2 was discussed and proposed.

2. Experimental Section

2.1. Preparation of Photocatalysts. N-doped TiO_2 (N-TiO_2) was prepared by partial oxidation of TiN. In a typical process, 3.0 g TiN powder was loaded in a ceramic crucible, and then placed in the middle of muffle furnace open to the atmosphere. The temperature was slowly ramped up to 450°C at a rate of 15°C/min and kept for 2 h to obtain N-doped TiO_2. V_2O_5 cluster modification was performed by incipient wetness impregnation of N-doped TiO_2 with aqueous solutions of NH_4VO_3 at room temperature, followed by stirring for 1 h, treating at 150°C for water evaporation and heating at 300°C for 1 h. The amount of loaded vanadium was controlled at 0, 0.01, 0.05, 0.2, 0.5, and 1.0 wt.%. The as-prepared samples were labeled as N-TiO_2/V_2O_5–x, where x represented the content of vanadium. For comparison, V_2O_5 (vanadium: 0.5 wt.%) was also loaded on SiO_2 instead of N-doped TiO_2 by the same process. The reference sample was labeled as SiO_2/V_2O_5–0.5%. Pure V_2O_5 was prepared accordingly in the absence of N-doped TiO_2 and SiO_2.

2.2. Characterization. The crystal phase of the samples was analyzed by X-ray diffraction with Cu Kα radiation (XRD: model D/max RA, Rigaku Co., Japan). Raman spectra were recorded at room temperature using a micro-Raman spectrometer (Raman: RAMANLOG 6, USA) with a 514.5 nm Ar^+ laser as the excitation source in a backscattering geometry. The morphology and structure of the samples were examined by transmission electron microscopy (TEM: JEM-2010, Japan). X-ray photoelectron spectroscopy with Al Kα X-rays ($h\nu$ = 1486.6 eV) radiation (XPS: Thermo ESCALAB 250, USA) was used to investigate the surface properties of the samples. The shift of the binding energy was corrected using the C1s level at 284.8 eV as an internal standard. The UV-vis diffuse reflection spectra were obtained for the dry-pressed disk samples using a Scan UV-vis spectrophotometer (UV-vis DRS: UV-2450, Japan) equipped with an integrating sphere assembly, using $BaSO_4$ as reflectance sample. The photoluminescence spectra were measured with a fluorospectrophotometer (PL: Fluorolog-3-Tau, France) using a Xe lamp as excitation source with optical filter. Nitrogen adsorption-desorption isotherms were obtained on a nitrogen adsorption apparatus (ASAP 2020, USA) with all samples degassed at 200°C prior to measurements. The BET surface area was determined by a multipoint BET method using the adsorption data in the relative pressure (P/P_0) range of 0.05–0.3.

2.3. Visible Light Photocatalytic Activity. The visible light photocatalytic activity was evaluated by removal of toluene in air in a continuous flow reactor at ambient temperature. The volume of the rectangular reactor, made of stainless steel and covered with Saint-Glass, was 4.5 L (30 cm × 15 cm × 10 cm). A 300 W commercial Xe lamp was vertically placed outside the reactor. Four minifans were used to cool the lamp. For the visible light photocatalytic activity test, a UV cut-off filter (420 nm) was adopted to remove UV light in the light beam. Photocatalyst (0.20 g) was coated onto a dish with a diameter of 12.0 cm. The coated dish was then treated at 70°C to remove water in the suspension. The toluene gas was acquired from a compressed gas cylinder at a concentration of 100 ppm of toluene. The initial concentration of toluene was diluted to 1.0 ppm at indoor level by the air stream supplied by compressed gas cylinder. The relative humidity (RH) level of the flow system was controlled at 50%. The gas streams were premixed completely by a gas blender, and the flow rate was controlled at 1.0 L/min by a mass flow controller. After the adsorption-desorption equilibrium was achieved, the lamp was turned on. The concentration of toluene was continuously measured by GC-FID (Shanghai, 7890II). The removal ratio (η) of toluene was calculated as $\eta(\%) = (1 - C/C_0) \times 100\%$, where C and C_0 are concentrations of toluene in the outlet steam and the feeding stream, respectively. The kinetics of photocatalytic toluene removal reaction is a pseudo first-order reaction as $\ln(C_0/C) = kt$, where k is the initial apparent rate constant [44, 45].

3. Results and Discussion

3.1. Phase Structure. The XRD patterns of as-prepared samples are shown in Figure 1. The phase structure of N-TiO_2 and V_2O_5 cluster-modified N-TiO_2 samples consists of mixed phases of anatase (JCPDS file No. 21–1272) and rutile (JCPDS, file no. 77–442). In the absence of substrate N-TiO_2, pure orthorhombic V_2O_5 phase (JSPD file no. 72–433) was produced. No characteristic diffraction peaks of V_2O_5 are observed in N-TiO_2/V_2O_5 composite samples because of its lower loading content, on the other hand, also indicating that V_2O_5 clusters were well dispersed on the N-TiO_2 surface [34, 35]. Figure 1 also shows that V_2O_5 cluster loading has almost no influence on the phase structure of N-TiO_2. By using the Debye-Scherrer equation, the crystallite sizes of anatase and rutile phase are calculated to be 18.3 and 22.8 nm, respectively. The BET surface areas of N-doped TiO_2 are measured to be 62.8 cm^2/g, and V_2O_5 cluster loading is found to have little influence on the surface areas of N-doped TiO_2.

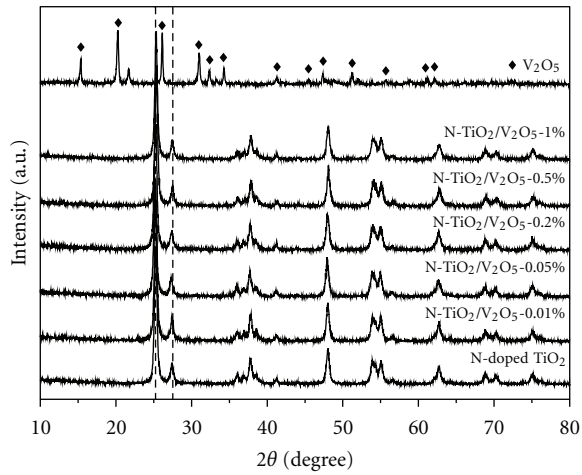

Figure 1: XRD patterns of N-doped TiO_2, V_2O_5 cluster modified N-TiO_2 and V_2O_5 samples.

3.2. Raman Analysis. Figure 2(a) shows the Raman spectra of N-doped TiO_2, selected V_2O_5 cluster modified N-TiO_2, and V_2O_5 samples. The observed characteristic Raman bands at 144, 196, 395, 515, and 638 cm^{-1} for samples containing N-TiO_2, assigned to the E_g, B_{1g}, A_{1g}, B_{2g}, and E_g vibrational modes of anatase phase TiO_2 [46]. The typical Raman bands of rutile phase TiO_2 appear at 143, 235, 447, and 612 cm^{-1}, which can be ascribed to the B_{1g}, two-phonon scattering, E_g, and A_{1g} modes of rutile phase, respectively [47]. Raman bands of rutile phase at 143 cm^{-1} are overlapped by 144 cm^{-1} band of anatase phase. The inset in Figure 2(a) shows the enlarged Raman bands at 447 cm^{-1} of rutile phase for samples containing N-TiO_2. As the content of rutile phase is low, other Raman bands of rutile phase cannot be observed directly in Figure 2(a). Raman mode of V_2O_5 is also shown in Figure 2(a) [48]. No Raman bands relevant to V_2O_5 are observed for the composite samples, which imply the absence of a separate crystalline V_2O_5 phase on the N-TiO_2/V_2O_5 samples, consistent with XRD results. The enlarged view of Raman bands in the range of 110–180 cm^{-1} in Figure 2(b) shows that the bands at 144 cm^{-1} shift to lower wave numbers as the loading content of V_2O_5 increases, suggesting the strong interaction between N-TiO_2 and V_2O_5 clusters.

3.3. TEM-EDS Analysis. TEM observation (Figures 3(a) and 3(b)) reveals that the N-TiO_2 and N-TiO_2/V_2O_5-0.5% sample consists of agglomerates of primary particles of 20–30 nm in diameter. For V_2O_5 modified sample, some V_2O_5 clusters with size of ca. 1–3 nm are observed and dispersed on the surface of N-TiO_2 (Figure 3(b) and see Figure S1 in supplementary material available on line at doi: 10.1155/2012/569716). The direct contact between V_2O_5 cluster and N-TiO_2 favors the formation of heterojunction between the two components. Figure 3(c) illustrates the energy-dispersive X-ray spectroscopy (EDS) spectra of N-TiO_2/V_2O_5-0.5% sample. The amount of vanadium content obtained from EDS (Table inset in Figure 3(c)) is in agreement with the modification content. To further reveal the dispersity of V_2O_5 clusters, elemental mapping images of O, Ti, and V are demonstrated in Figures 3(d)–3(f). It can be seen that V_2O_5 clusters are uniformly deposited on the surface of N-TiO_2 nanoparticles, which is also favorable for the interaction between V_2O_5 clusters and N-TiO_2.

3.4. XPS Analysis. XPS is used to determine the chemical composition and surface properties of catalysts. Figure 4(a) shows the binding energy (E_b) for the N1s region of N-TiO_2 and N-TiO_2/V_2O_5-0.5% samples. For both samples, E_b of N1s at around 400 eV can be observed. This E_b is a typical feature of substitutional lattice nitrogen (N^{3-}) for oxygen, forming N-Ti-O structure [43]. The formation of N-Ti-O bond is the natural result of partial oxidation of TiN by oxygen. The content of doped nitrogen is determined to be 0.87 at % and have little change after modification with V_2O_5 clusters according to the XPS result.

Figure 4(b) shows the XPS spectra for O1s region. It can be seen that the O1s region can be fitted into three peaks for both samples, which can be attributed to Ti-O (529.9 eV), -OH hydroxyl groups (531.3 eV), and chemisorbed H_2O (532.7 eV), respectively [44]. Further observation in Figure 4(b) indicates that the molar ratio of oxygen in hydroxyl groups to all kinds of oxygen contributions increases after V_2O_5 cluster modification.

Figure 4(c) shows the E_b for Ti $2p_{3/2}$ for both samples. It can be seen that Ti2p peak at 458.85 eV of N-TiO_2/V_2O_5-0.5% sample shifted positively by 0.25 eV in comparison with that of the Ti2p peak in N-TiO_2 sample (458.60 eV). The shifting of E_b can be ascribed to the interaction between host N-TiO_2 and guest V_2O_5 clusters, as also confirmed by Raman spectra [20].

Figure 4(d) shows the E_b for $V2p_{3/2}$ for both samples. The V $2p_{3/2}$ peak of V_2O_5 cluster samples can be fitted into two peaks, located at 517.3 and 516.2 eV. These two E_b can be assigned to V^{5+} and V^{4+}, respectively [49]. The variation of vanadium oxidation state is frequently observed in catalysis. In XPS measurement, N-TiO_2 can be exited by the high energy of X-rays ($h\nu$ = 1486.6 eV) to produced electrons in conduction band (CB). The V^{5+} then accepts the CB electrons to produce V^{4+}. These results also confirm that the electrons transfer from the CB of N-TiO_2 to V_2O_5 clusters on the surface and the partial reduction of V^{5+} to V^{4+} [37].

3.5. UV-Vis DRS. Figure 5(a) shows UV-vis DRS of N-doped TiO_2, N-TiO_2/V_2O_5, and V_2O_5 samples and P25. Compared with undoped TiO_2 P25, optical absorption of N-doped TiO_2 shifts into visible light region (400–550 nm) as the localized N doping level was formed in the band gap. When the amount of vanadium loaded was less than 0.20 wt.%, there was no obvious change in visible light absorption compared with N-TiO_2. The optical absorption in visible region was significantly increased when the content of vanadium loaded was higher than 0.50 wt.%. Pure V_2O_5 exhibits broad visible light absorption. The enhanced absorption of V_2O_5 cluster-modified N-TiO_2 nanocomposite can be ascribed to d-d transition of vanadium species.

Bandgap (E_g) energies can be estimated from UV-vis DRS spectra. Semiconductors are classified to be indirect or

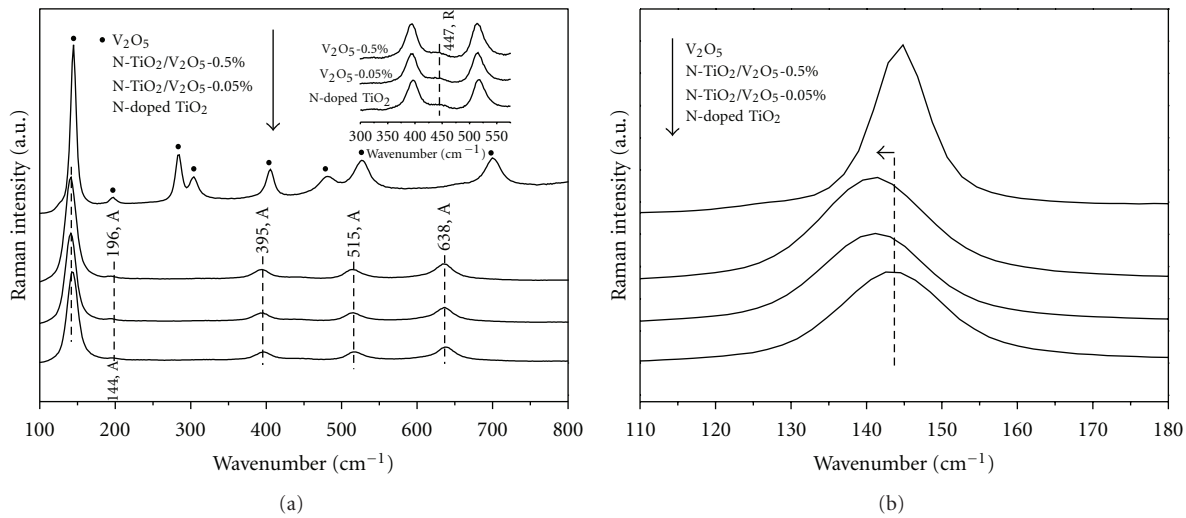

Figure 2: Raman spectra of N-doped TiO_2, selected V_2O_5 cluster modified N-TiO_2 and V_2O_5 samples (A: anatase, R: rutile).

direct according to the lowest allowed electronic transition. The relation between absorption coefficient (α) and incident photon energy ($h\nu$) can be written as $\alpha h\nu = B_d(h\nu - E_g)^n$ for allowed transitions ($n = 2$ for indirect transition, $n = 1/2$ direct transition), where B_d is the absorption constants. Plot of $(\alpha h\nu)^{1/2}$ and $(\alpha h\nu)^2$ versus $h\nu$ from the spectra data of N-TiO_2 and V_2O_5 in Figure 5(a) presented in Figure 5(b) [44, 45]. The E_g estimated from the intercept of the tangents to the plots is 2.75 and 2.24 eV for N-TiO_2 and V_2O_5, respectively. The estimated E_g for V_2O_5 is consistent with previous report [50]. It is generally recognized that nitrogen doping could reduce the bandgap of TiO_2 by uplifting the position of valence band (VB) while keeping the position of CB unchanged [15–18].

3.6. PL Spectra. Photoluminescence (PL) emission spectra have been widely used to investigate the efficiency of charge carrier trapping, migration, and transfer in order to understand the fate of electron/hole pairs in semiconductors since PL emission results from the recombination of photogenerated charge carriers. Figure 6 shows the room-temperature PL spectra of selected V_2O_5 cluster-modified N-TiO_2 samples under the excitation of 300 nm light and 425 nm light. As the PL emission reflects the recombination rate of excited electrons and holes, a lower PL intensity indicates decreased charge recombination rate and enhanced charge separation rate [17–20]. It can be seen from Figure 6 that the PL intensity of V_2O_5 cluster modified N-TiO_2 is lower than that of N-TiO_2. As the loading content of V_2O_5 increases, the PL intensity decreases correspondingly. This result indicates that V_2O_5 loaded on N-TiO_2 surface (Inset in Figure 2(a)) can effectively enhance the separation of electron/hole pairs. This also implies that N-TiO_2/V_2O_5 has a lower recombination rate of electron/hole pairs under both UV and visible light irradiation. This is ascribed to the fact that the electrons are excited from the VB to the CB of N-TiO_2 and then migrate to V_2O_5 clusters, which prevents the direct recombination of electrons and holes, as also confirmed by XPS result on V2p (Figure 4(d)).

3.7. Photocatalytic Activity and Proposed Mechanism. To elucidate the effects of V_2O_5 cluster modification on the photoactivity of N-doped TiO_2, visible light photocatalytic degradation of gaseous toluene at indoor level was performed. Figure 7 shows the visible light photocatalytic degradation curves (Figure 7(a)) and apparent reaction rate constant k (Figure 7(b)) of SiO_2/V_2O_5, N-TiO_2, and N-TiO_2/V_2O_5 samples with different loading content of V_2O_5. SiO_2/V_2O_5 exhibits negligible activity, which implies that V_2O_5 alone is not active under visible light probably due to the rapid recombination between CB electrons and VB holes. N-doped TiO_2 shows decent visible light activity toward toluene degradation with removal ratio η of 27.5% and k of 0.009 min^{-1}. With the loading of V_2O_5 clusters in rang of 0.01∼1.0 wt.%, N-TiO_2/V_2O_5 samples exhibit significantly enhanced visible light photocatalytic activity than that of unmodified N-TiO_2. After loading only 0.01 wt.% of V_2O_5 on N-TiO_2, the visible light activity of N-TiO_2/V_2O_5-0.01% is markedly enhanced with a η 39.7% and k of 0.0165 min^{-1}. With further increasing V_2O_5 loading from 0.01 wt.% to 0.5 wt.%, the visible light activity on N-TiO_2/V_2O_5 is further increased and achieves a maximum η of 52.4% and k of 0.027 min^{-1}. When the V_2O_5 loading content is higher than 0.5 wt.%, a further increase in V_2O_5 loading leads to a obvious reduction of the photocatalytic activity. This is probably due to the following reasons: (i) deposition of excessive V_2O_5 clusters resulted in the decrease (or shield) of the N-TiO_2 surface active sites; (ii) disappearance of surface effect due to the increase of particle size [34, 35].

From what has been observed and discussed above, several conclusions can be drawn: (1) V_2O_5 is inactive for photocatalytic degradation of toluene under visible light irradiation although the band gap of V_2O_5 is suitable for visible light excitation. (2) After V_2O_5 cluster modification, the visible light activities of N-TiO_2/V_2O_5 samples are highly

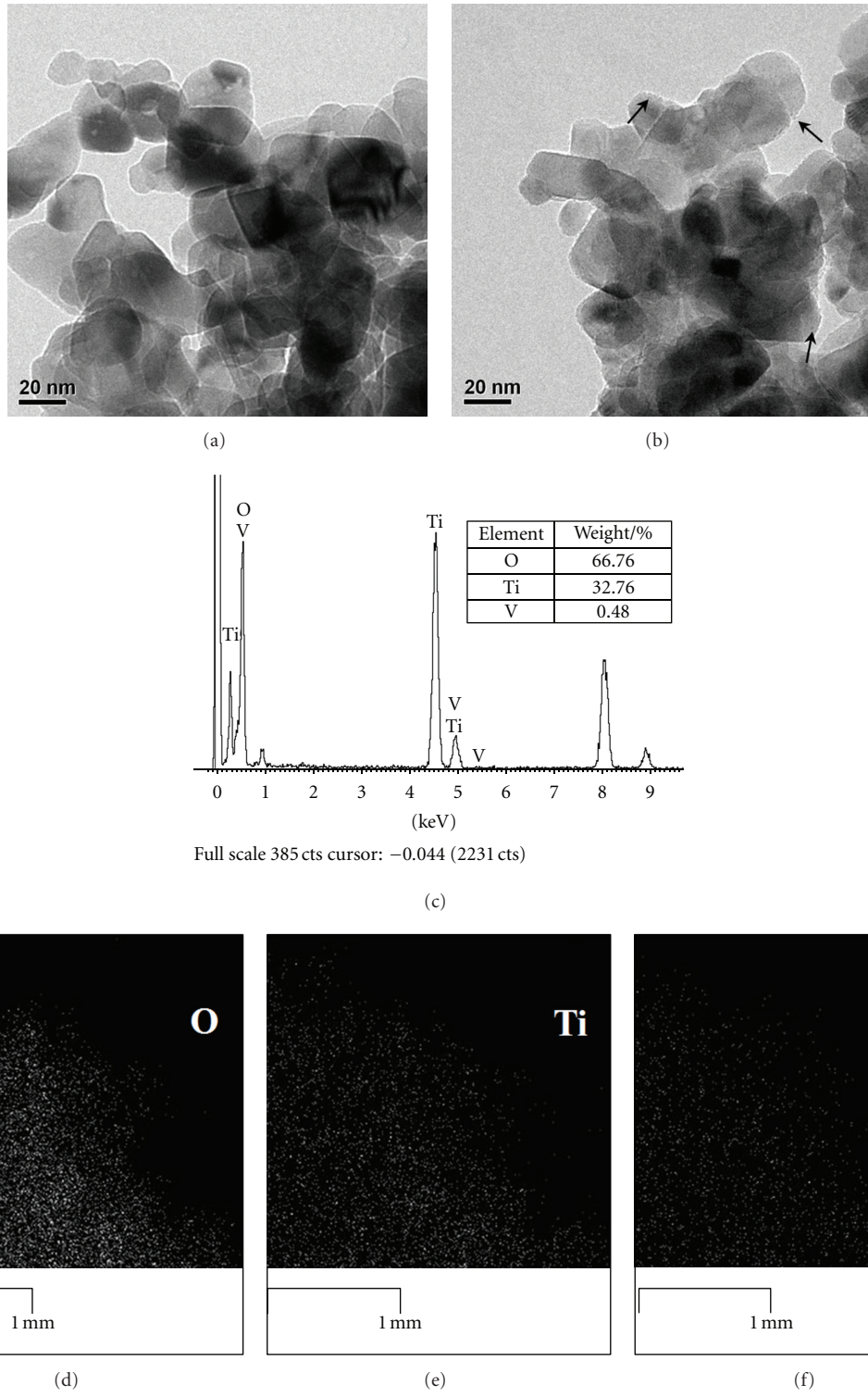

FIGURE 3: TEM image of N-doped TiO_2 sample (a), TEM image (b), EDS (c) and elemental mapping image (d, e, f) of of N-TiO_2/V_2O_5-0.5% sample.

enhanced. (3) The content of V_2O_5 cluster significantly influences visible light activity of N-TiO_2. Obviously, the enhanced separation of electrons and holes pairs on N-TiO_2/V_2O_5 nanocomposite due to the CB electron migration from N-TiO_2 to V_2O_5 cluster is directly responsible for the highly enhanced visible light photocatalytic activity.

Here comes a fundamental issue. What is the driven force for CB electron of N-TiO_2 to migrate to V_2O_5 clusters? The

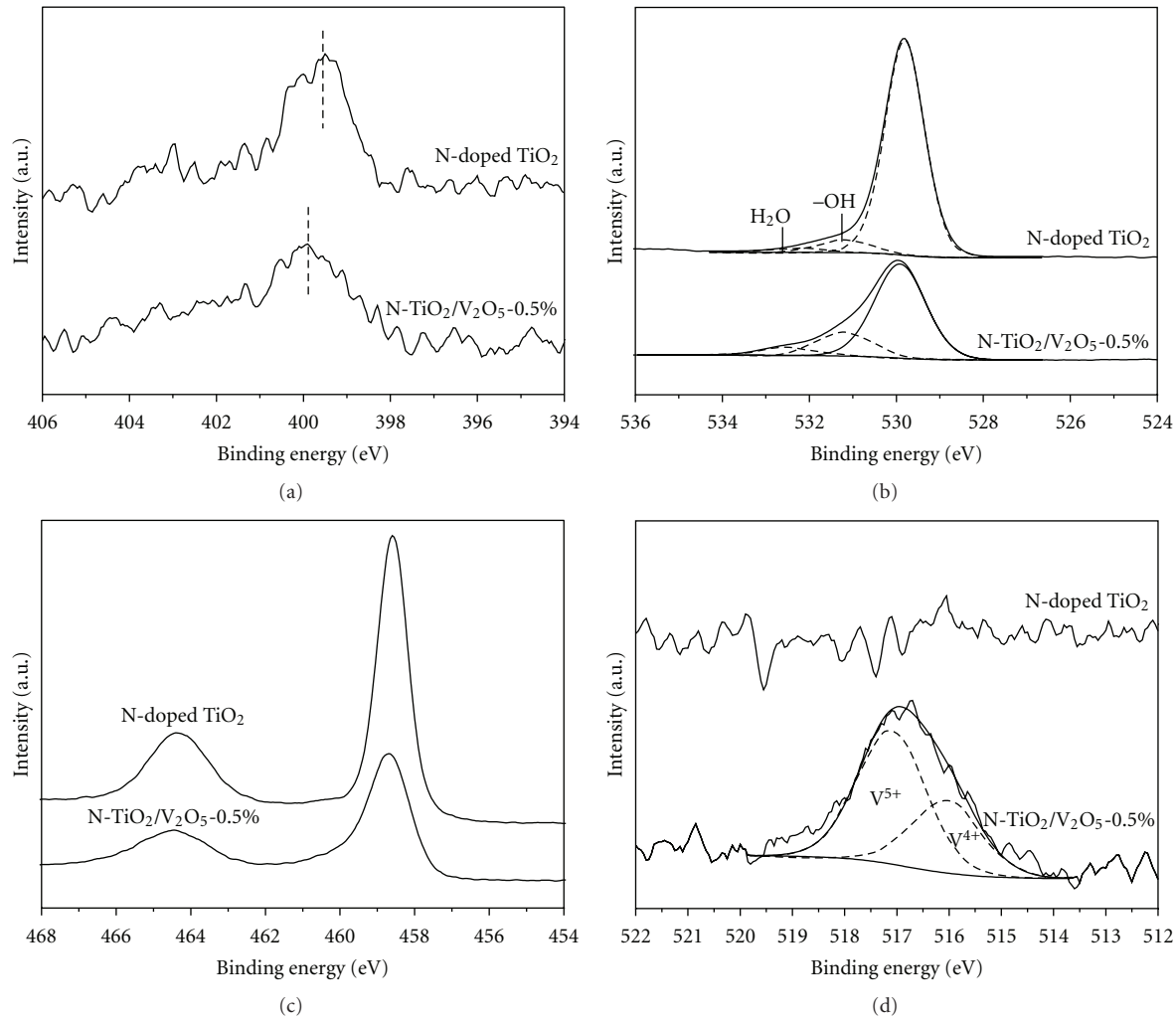

Figure 4: XPS spectra for N-doped TiO_2 and N-TiO_2/V_2O_5-0.5% samples of N1s (a), O1s (b), Ti2p, (c) and V2p (d).

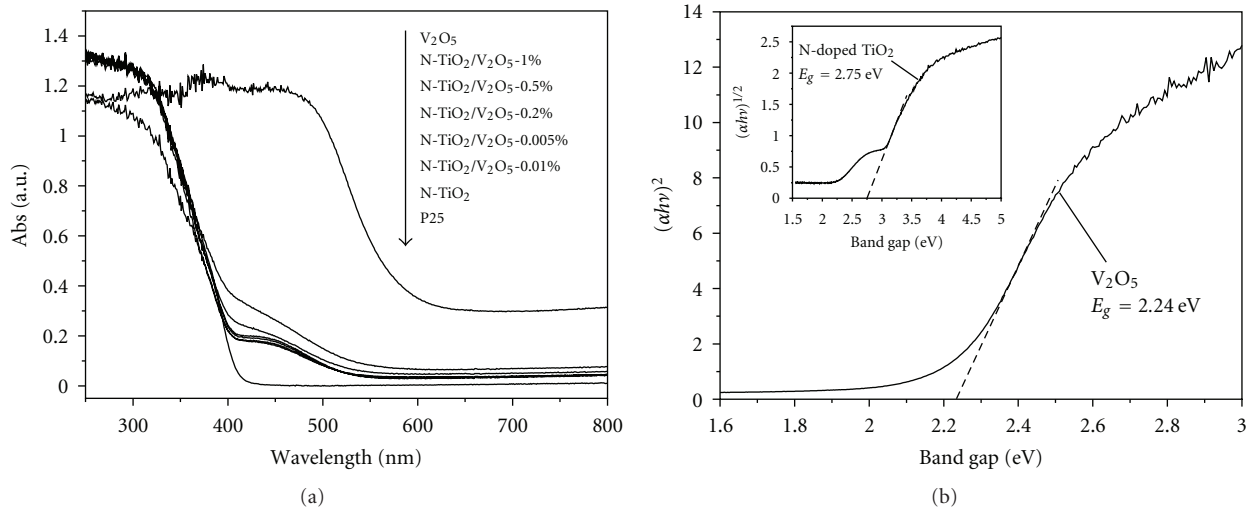

Figure 5: UV-vis DRS of N-doped TiO_2, N-TiO_2/V_2O_5, V_2O_5 samples and P25 (a). Plot of $(\alpha h\nu)^2$ versus photon energy of V_2O_5 (direct semiconductor) (b), inset in (b) shows the plot of $(\alpha h\nu)^{1/2}$ versus photon energy of N-TiO_2 (indirect semiconductor).

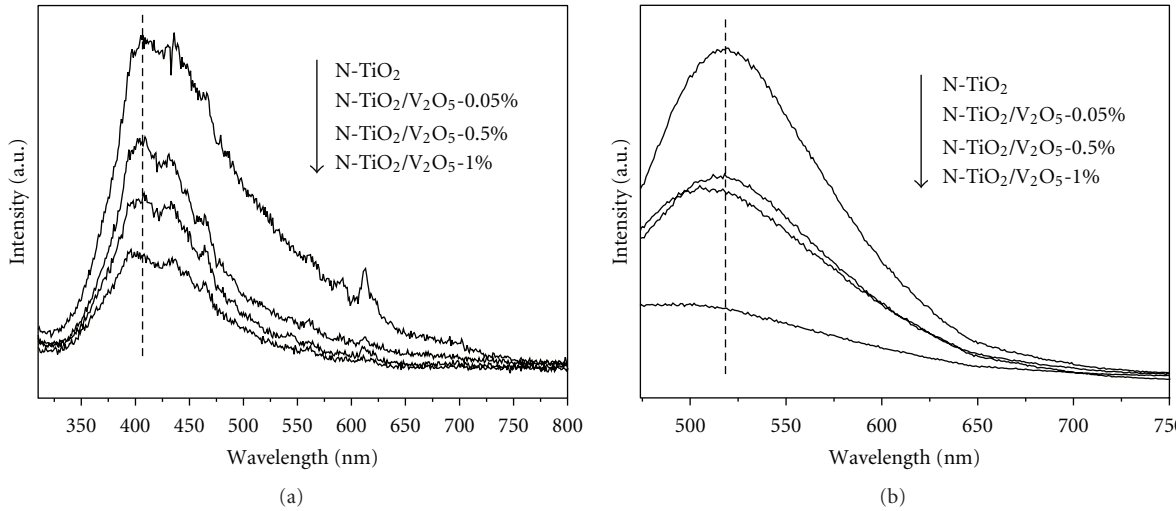

Figure 6: PL spectra of N-TiO_2 and selected V_2O_5 cluster modified N-TiO_2 samples under the excitation of 300 nm light (a) and 425 nm light (b).

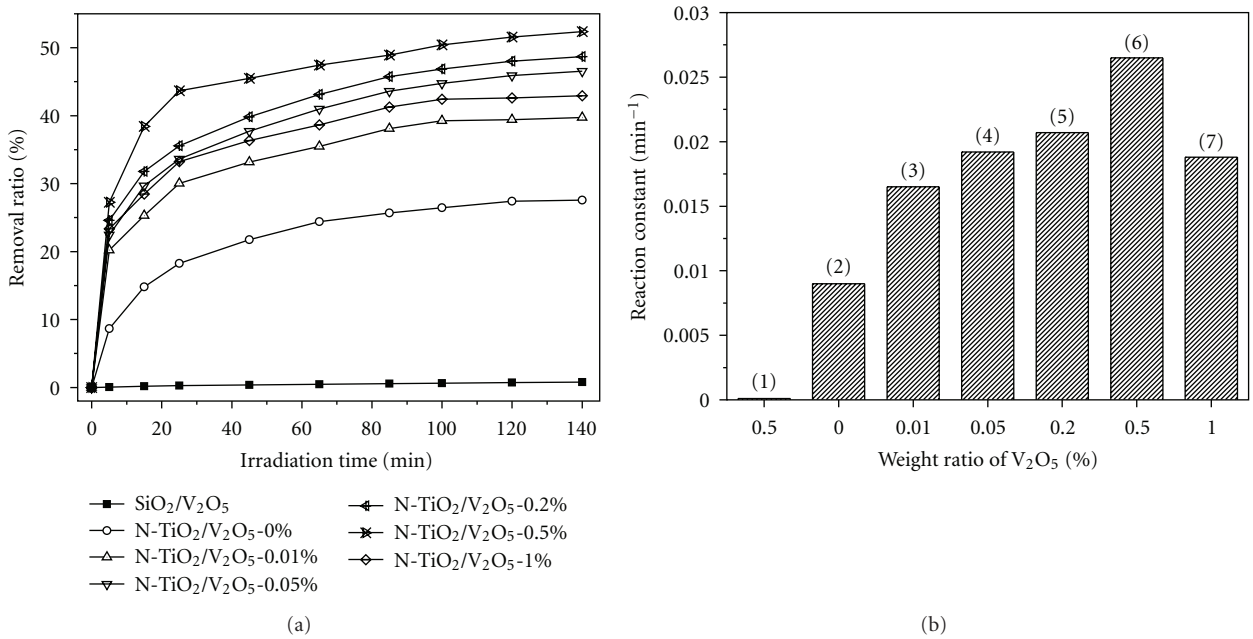

Figure 7: Visible light photocatalytic degradation curves (a) and comparison of the apparent rate constant (k) of as-prepared samples (b), (1) SiO_2/V_2O_5 sample, (2) N-TiO_2, (3)–(7) V_2O_5 cluster modified N-TiO_2 samples.

band edge positions of CB and VB of semiconductor can be determined with the following approach. The CB edge (E^0_{CB}) of a semiconductor at the point of zero charge (pH_{ZPC}) can be predicted by the equation $E^0_{CB} = X - E^C - 1/2E_g$ [35, 50], where X is the absolute electronegativity of the semiconductor (for V_2O_5, X is 6.10 eV [51]; for P25 TiO_2, X is 5.81 eV [51]; X is unknown for N-doped TiO_2). E_C is the energy of free electrons on the hydrogen scale (~4.5 eV). E_g is the band gap energy of the semiconductor. The calculated positions of CB and VB of V_2O_5 and P25 are listed in Table 1. It is well known that nonmetal doping does not change the CB position of TiO_2. The VB position of N-doped TiO_2 can be determined based on the calculated CB position of undoped TiO_2 P25 and E_g of N-doped TiO_2, as also shown in Table 1.

The schematic enhanced charge transfer and separation in the V_2O_5 cluster modified N-doped TiO_2 system are illustrated in Figure 8. Under visible light irradiation, electrons can be excited to the CB of N-TiO_2, leaving holes in the VB (1). These holes will react with OH^- on the catalyst surface to form •OH radicals (2). Because the potential of V_2O_5 (E^0_{CB} = 0.48 eV) is lower than the CB level of N-TiO_2 (E^0_{CB} = −0.19 V), the photogenerated CB electrons in N-TiO_2 can transfer rapidly to V_2O_5 clusters and then effectively reduce

Table 1: Absolute electronegativity, calculated conduction band (CB) edge, calculated valence band (VB) position, and bandgap energy for P25, V_2O_5, and N-doped TiO_2 at the point of zero charge.

Semiconductors	Absolute electronegativity (X) (/eV)	Calculated CB position (/eV)	Calculated VB position (/eV)	Band gap energy E_g (/eV)
P25	5.81	−0.19	2.81	3.0
V_2O_5	6.10	0.48	2.72	2.24
N-doped TiO_2	—	−0.19	2.56	2.75

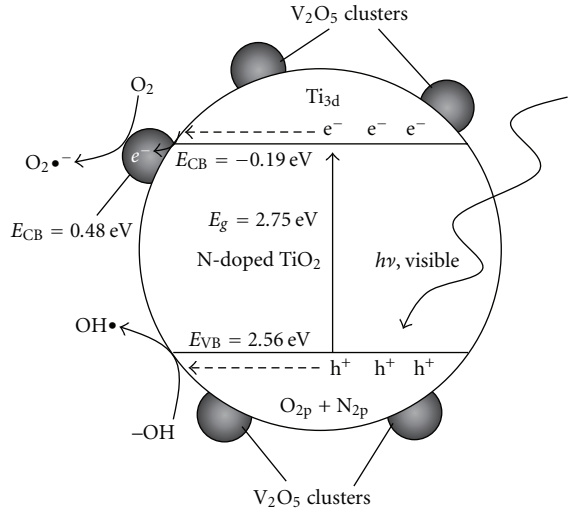

Figure 8: Schematic illustration for the enhanced charge transfer and separation in the V_2O_5 cluster modified N-doped TiO_2 system under visible light irradiation.

partial V^{5+} to V^{4+} (see Figure 4(d)), thus promoting the separation of and transfer of photogenerated electrons and holes pairs. The PL experiments further confirm the transfer of photogenerated electrons from N-TiO_2 to V_2O_5 clusters (Figure 6). The electrons accepted by V^{5+} can then be transferred quickly to oxygen molecules under the aerated condition to regenerate V^{4+} to produce $O_2^{\bullet-}$ superoxide anion radicals. The process can be defined as V^{5+}/V^{4+} redox cycle, as shown in the following equations (3)-(4):

$$\text{N-TiO}_2 + \nu\ (\text{visible}) \longrightarrow \text{h}^+ + \text{e}^- \quad (1)$$

$$\text{OH}^- + \text{h}^+ \longrightarrow \bullet\text{OH} \quad (2)$$

$$\text{V}^{5+}\ (\text{V}_2\text{O}_5) + \text{e}^- \longrightarrow \text{V}^{4+} \quad (3)$$

$$\text{V}^{4+} + \text{O}_2 \longrightarrow \text{V}^{5+}\ (\text{V}_2\text{O}_5) + \text{O}_2^{\bullet-}. \quad (4)$$

The •OH and $O_2^{\bullet-}$ radicals are known to be the most oxidizing species in photocatalysis reaction [1–3]. These results suggest that the separation of electrons and holes can be effectively enhanced by V_2O_5 clusters, which will greatly enhance the visible light photocatalytic activity of N-doped TiO_2. Similar phenomena have also been observed on CuO, $Cu(OH)_2$, and $Ni(OH)_2$ cluster modified TiO_2 with highly enhanced photocatalytic activity [34–36].

The effect of V_2O_5 cluster modification on the charge transfer and separation of other semiconductor is, to some extent, similar to that of the role of noble metals in photocatalysis [45, 52–54]. The present work not only displays a feasible route for the utilization of low cost V_2O_5 clusters as a substitute for noble metals in enhancing the photocatalysis but also demonstrates a facile method for preparation of highly active composite photocatalysts for environmental application.

4. Conclusion

In order to enhance the visible light photocatalytic activity of N-doped TiO_2 for practical environmental application, a facile impregnation-calcination method is developed for the preparation of highly active V_2O_5 cluster modified N-doped TiO_2 nanocomposites photocatalyst for degradation of toluene in air. The V_2O_5 clusters can act as electron mediator to effectively inhibit the recombination of photogenerated electron/hole pairs. The optimal V_2O_5 loading content is determined to be 0.5 wt.%, and the corresponding toluene removal ratio is 52.4%, which largely exceeds that of unmodified N-doped TiO_2. The CB potential of V_2O_5 (0.48 eV) is lower than the CB level of N-doped TiO_2 (−0.19 V), which is the driven force for the electron transfer from CB of N-doped TiO_2 to V_2O_5 clusters, thus greatly promoting the visible light activity of N-doped TiO_2. This work not only provides a feasible route for utilizing low-cost V_2O_5 clusters as a substitute for noble metals in enhancing the visible light photocatalysis but also demonstrates a facile method for preparation of highly active composites photocatalyst for large scale application.

Acknowledgment

This research is financially supported by the National Natural Science Foundation of China (51108487), the Program for Young Talented Teachers in Universities (Chongqing, 2011), the National High Technology Research and Development Program (863 Program) of China (2010AA064905), The key discipline development project of CTBU (1252001), Projects from Chongqing Education Commission (KJTD201020, KJZH11214, KJ090727), and Natural Science Foundation of Chongqing (CSTC, 2010BB0260).

References

[1] C. Chen, W. Ma, and J. Zhao, "Semiconductor-mediated photodegradation of pollutants under visible-light irradiation," *Chemical Society Reviews*, vol. 39, no. 11, pp. 4206–4219, 2010.

[2] A. V. Emeline, V. N. Kuznetsov, V. K. Rybchuk, and N. Serpone, "Visible-light-active titania photocatalysts: the case of N doped TiO_2-properties and some fundamental issues," *International Journal of Photoenergy*, vol. 2008, Article ID 258394, 19 pages, 2008.

[3] J. Mo, Y. Zhang, Q. Xu, J. J. Lamson, and R. Zhao, "Photocatalytic purification of volatile organic compounds in indoor air: a literature review," *Atmospheric Environment*, vol. 43, no. 14, pp. 2229–2246, 2009.

[4] S. Liu, J. Yu, and M. Jaroniec, "Anatase TiO_2 with dominant high-energy 001 facets: synthesis, properties, and applications," *Chemistry of Materials*, vol. 23, no. 18, pp. 4085–4093, 2011.

[5] H. Zhang, G. Chen, and D. W. Bahnemann, "Photoelectrocatalytic materials for environmental applications," *Journal of Materials Chemistry*, vol. 19, no. 29, pp. 5089–5121, 2009.

[6] X. Chen, S. Shen, L. Guo, and S. S. Mao, "Semiconductor-based photocatalytic hydrogen generation," *Chemical Reviews*, vol. 110, no. 11, pp. 6503–6570, 2010.

[7] D. Zhang, G. Li, and J. C. Yu, "Inorganic materials for photocatalytic water disinfection," *Journal of Materials Chemistry*, vol. 20, no. 22, pp. 4529–4536, 2010.

[8] X. Nie, S. Zhuo, G. Maeng, and K. Sohlberg, "Doping of TiO_2 polymorphs for altered optical and photocatalytic properties," *International Journal of Photoenergy*, vol. 2009, Article ID 294042, 22 pages, 2009.

[9] R. Asahi, T. Morikawa, T. Ohwaki, K. Aoki, and Y. Taga, "Visible-light photocatalysis in nitrogen-doped titanium oxides," *Science*, vol. 293, no. 5528, pp. 269–271, 2001.

[10] S. U. M. Khan, M. Al-Shahry, and W. B. Ingler, "Efficient photochemical water splitting by a chemically modified n-TiO_2," *Science*, vol. 297, no. 5590, pp. 2243–2245, 2002.

[11] S. Sakthivel and H. Kisch, "Daylight photocatalysis by carbon-modified titanium dioxide," *Angewandte Chemie*, vol. 42, no. 40, pp. 4908–4911, 2003.

[12] Y. Huang, W. Ho, S. Lee, L. Zhang, G. Li, and J. C. Yu, "Effect of carbon doping on the mesoporous structure of nanocrystalline titanium dioxide and its solar-light-driven photocatalytic degradation of NOx," *Langmuir*, vol. 24, no. 7, pp. 3510–3516, 2008.

[13] W. Haiqiang, W. Zhongbiao, and L. Yue, "A simple two-step template approach for preparing carbon-doped mesoporous TiO_2 hollow microspheres," *Journal of Physical Chemistry C*, vol. 113, no. 30, pp. 13317–13324, 2009.

[14] Z. Ai, L. Zhu, S. Lee, and L. Zhang, "NO treated TiO_2 as an efficient visible light photocatalyst for NO removal," *Journal of Hazardous Materials*, vol. 192, no. 1, pp. 361–367, 2011.

[15] Y. Cong, J. Zhang, F. Chen, and M. Anpo, "Synthesis and characterization of nitrogen-doped TiO_2 nanophotocatalyst with high visible light activity," *Journal of Physical Chemistry C*, vol. 111, no. 19, pp. 6976–6982, 2007.

[16] K. Yang, Y. Dai, and B. Huang, "Density functional study of boron-doped anatase TiO_2," *Journal of Physical Chemistry C*, vol. 114, no. 46, pp. 19830–19834, 2010.

[17] X. Chen, X. Wang, Y. Hou, J. Huang, L. Wu, and X. Fu, "The effect of postnitridation annealing on the surface property and photocatalytic performance of N-doped TiO_2 under visible light irradiation," *Journal of Catalysis*, vol. 255, no. 1, pp. 59–67, 2008.

[18] F. Dong, W. Zhao, Z. Wu, and S. Guo, "Band structure and visible light photocatalytic activity of multi-type nitrogen doped TiO_2 nanoparticles prepared by thermal decomposition," *Journal of Hazardous Materials*, vol. 162, no. 2-3, pp. 763–770, 2009.

[19] Y. Cong, J. Zhang, F. Chen, M. Anpo, and D. He, "Preparation, photocatalytic activity, and mechanism of nano-TiO_2 Co-doped with nitrogen and iron (III)," *Journal of Physical Chemistry C*, vol. 111, no. 28, pp. 10618–10623, 2007.

[20] F. Dong, H. Wang, Z. Wu, and J. Qiu, "Marked enhancement of photocatalytic activity and photochemical stability of N-doped TiO_2 nanocrystals by Fe^{3+}/Fe^{2+} surface modification," *Journal of Colloid and Interface Science*, vol. 343, no. 1, pp. 200–208, 2010.

[21] J. Lu, Y. Dai, H. Jin, and B. Huang, "Effective increasing of optical absorption and energy conversion efficiency of anatase TiO_2 nanocrystals by hydrogenation," *Physical Chemistry Chemical Physics*, vol. 13, no. 40, pp. 18063–18068, 2011.

[22] J. Zhang, Y. Wu, M. Xing, S. A. K. Leghari, and S. Sajjad, "Development of modified N doped TiO_2 photocatalyst with metals, nonmetals and metal oxides," *Energy and Environmental Science*, vol. 3, no. 6, pp. 715–726, 2010.

[23] F. Dong, W. Zhao, and Z. Wu, "Characterization and photocatalytic activities of C, N and S co-doped TiO_2 with 1D nanostructure prepared by the nano-confinement effect," *Nanotechnology*, vol. 19, no. 36, Article ID 365607, 2008.

[24] P. Periyat, D. E. McCormack, S. J. Hinder, and S. C. Pillai, "One-pot synthesis of anionic (nitrogen) and cationic (sulfur) codoped high-temperature stable, visible light active, anatase Photocatalysts," *Journal of Physical Chemistry C*, vol. 113, no. 8, pp. 3246–3253, 2009.

[25] Y. huo, Y. jin, J. zhu, and H. li, "Highly active $TiO_{2-x-y}N_xF_y$ visible photocatalyst prepared under supercritical conditions in NH_4F/EtOH fluid," *Applied Catalysis B*, vol. 89, no. 3-4, pp. 543–550, 2009.

[26] M. Xing, J. Zhang, and F. Chen, "Photocatalytic performance of N-doped TiO_2 adsorbed with Fe^{3+} ions under visible light by a redox treatment," *Journal of Physical Chemistry C*, vol. 113, no. 29, pp. 12848–12853, 2009.

[27] H. Wei, Y. Wu, N. Lun, and F. Zhao, "Preparation and photocatalysis of TiO_2 nanoparticles co-doped with nitrogen and lanthanum," *Journal of Materials Science*, vol. 39, no. 4, pp. 1305–1308, 2004.

[28] D. E. Gu, B. C. Yang, and Y. D. Hu, "V and N co-doped nanocrystal anatase TiO_2 photocatalysts with enhanced photocatalytic activity under visible light irradiation," *Catalysis Communications*, vol. 9, no. 6, pp. 1472–1476, 2008.

[29] L. H. Huang, C. Sun, and Y. L. Liu, "Pt/N-codoped TiO_2 nanotubes and its photocatalytic activity under visible light," *Applied Surface Science*, vol. 253, no. 17, pp. 7029–7035, 2007.

[30] Y. Wu, H. Liu, J. Zhang, and F. Chen, "Enhanced photocatalytic activity of nitrogen-doped titania by deposited with gold," *Journal of Physical Chemistry C*, vol. 113, no. 33, pp. 14689–14695, 2009.

[31] B. Gao, Y. Ma, Y. Cao, W. Yang, and J. Yao, "Great enhancement of photocatalytic activity of nitrogen-doped titania by coupling with tungsten oxide," *Journal of Physical Chemistry B*, vol. 110, no. 29, pp. 14391–14397, 2006.

[32] Q. Li, N. J. Easter, and J. K. Shang, "As(III) removal by palladium-modified nitrogen-doped titanium oxide nanoparticle photocatalyst," *Environmental Science and Technology*, vol. 43, no. 5, pp. 1534–1539, 2009.

[33] X. C. Wang, J. C. Yu, Y. Chen, L. Wu, and X. Z. Fu, "ZrO_2-modified mesoporous manocrystalline $TiO_{2-x}N_x$ as efficient

visible light photocatalysts," *Environmental Science & Technology*, vol. 40, no. 7, pp. 2369–2374, 2006.

[34] J. Yu, Y. Hai, and B. Cheng, "Enhanced photocatalytic H_2-production activity of TiO_2 by $Ni(OH)_2$ cluster modification," *Journal of Physical Chemistry C*, vol. 115, no. 11, pp. 4953–4958, 2011.

[35] J. Yu and J. Ran, "Facile preparation and enhanced photocatalytic H_2-production activity of $Cu(OH)_2$ cluster modified TiO_2," *Energy and Environmental Science*, vol. 4, no. 4, pp. 1364–1371, 2011.

[36] M. Liu, X. Qiu, M. Miyauchi, and K. Hashimoto, "Cu(II) oxide amorphous nanoclusters grafted Ti^{3+} self-doped TiO_2: an efficient visible light photocatalyst," *Chemistry of Materials*, vol. 23, no. 23, pp. 5282–5286, 2011.

[37] Z. Wu, F. Dong, Y. Liu, and H. Wang, "Enhancement of the visible light photocatalytic performance of C-doped TiO_2 by loading with V_2O_5," *Catalysis Communications*, vol. 11, no. 2, pp. 82–86, 2009.

[38] M. A. Rauf, S. B. Bukallah, A. Hamadi, A. Sulaiman, and F. Hammadi, "The effect of operational parameters on the photoinduced decoloration of dyes using a hybrid catalyst V_2O_5/TiO_2," *Chemical Engineering Journal*, vol. 129, no. 1–3, pp. 167–172, 2007.

[39] K. Bhattacharyya, S. Varma, A. K. Tripathi, S. R. Bharadwaj, and A. K. Tyagi, "Effect of vanadia doping and its oxidation state on the photocatalytic activity of TiO_2 for gas-phase oxidation of ethene," *Journal of Physical Chemistry C*, vol. 112, no. 48, pp. 19102–19112, 2008.

[40] S. Higashimoto, W. Tanihata, Y. Nakagawa, M. Azuma, H. Ohue, and Y. Sakata, "Effective photocatalytic decomposition of VOC under visible-light irradiation on N-doped TiO_2 modified by vanadium species," *Applied Catalysis A*, vol. 340, no. 1, pp. 98–104, 2008.

[41] D. Bi and Y. Xu, "Improved photocatalytic activity of WO_3 through clustered Fe_2O_3 for organic degradation in the presence of H_2O_2," *Langmuir*, vol. 27, no. 15, pp. 9359–9366, 2011.

[42] Q. Li, B. Guo, J. Yu et al., "Highly efficient visible-light-driven photocatalytic hydrogen production of CdS-cluster-decorated graphene nanosheets," *Journal of the American Chemical Society*, vol. 133, no. 28, pp. 10878–10884, 2011.

[43] Z. Wu, F. Dong, W. Zhao, and S. Guo, "Visible light induced electron transfer process over nitrogen doped TiO_2 nanocrystals prepared by oxidation of titanium nitride," *Journal of Hazardous Materials*, vol. 157, no. 1, pp. 57–63, 2008.

[44] F. Dong, S. Guo, H. Wang, X. Li, and Z. Wu, "Enhancement of the visible light photocatalytic activity of C-doped TiO_2 nanomaterials prepared by a green synthetic approach," *Journal of Physical Chemistry C*, vol. 115, no. 27, pp. 13285–13292, 2011.

[45] F. Dong, H. Wang, G. Sen, Z. Wu, and S. C. Lee, "Enhanced visible light photocatalytic activity of novel Pt/C-doped TiO_2/$PtCl_4$ three-component nanojunction system for degradation of toluene in air," *Journal of Hazardous Materials*, vol. 187, no. 1–3, pp. 509–516, 2011.

[46] Y. Su, J. Yu, and J. Lin, "Vapor-thermal preparation of highly crystallized TiO_2 powder and its photocatalytic activity," *Journal of Solid State Chemistry*, vol. 180, no. 7, pp. 2080–2087, 2007.

[47] J. Zhang, M. Li, Z. Feng, J. Chen, and C. Li, "UV raman spectroscopic study on TiO_2 I. phase transformation at the surface and in the bulk," *Journal of Physical Chemistry B*, vol. 110, no. 2, pp. 927–935, 2006.

[48] F. Chen, J. Wang, J. Q. Xu, and X. P. Zhou, "Visible light photodegradation of organic compounds over V_2O_5/MgF_2 catalyst," *Applied Catalysis A*, vol. 348, no. 1, pp. 54–59, 2008.

[49] M. Heber and W. Grünert, "Application of ultraviolet photoelectron spectroscopy in the surface characterization of polycrystalline oxide catalysts. 2. Depth variation of the reduction degree in the surface region of partially reduced V_2O_5," *Journal of Physical Chemistry B*, vol. 104, no. 22, pp. 5288–5297, 2000.

[50] H. Jiang, M. Nagai, and K. Kobayashi, "Enhanced photocatalytic activity for degradation of methylene blue over V_2O_5/$BiVO_4$ composite," *Journal of Alloys and Compounds*, vol. 479, no. 1-2, pp. 821–827, 2009.

[51] X. Yong and M. A. A. Schoonen, "The absolute energy positions of conduction and valence bands of selected semiconducting minerals," *American Mineralogist*, vol. 85, no. 3-4, pp. 543–556, 2000.

[52] H. Park, W. Choi, and M. R. Hoffmann, "Effects of the preparation method of the ternary CdS/TiO_2/Pt hybrid photocatalysts on visible light-induced hydrogen production," *Journal of Materials Chemistry*, vol. 18, no. 20, pp. 2379–2385, 2008.

[53] H. Tada, T. Mitsui, T. Kiyonaga, T. Akita, and K. Tanaka, "All-solid-state Z-scheme in CdS-Au-TiO_2 three-component nanojunction system," *Nature Materials*, vol. 5, no. 10, pp. 782–786, 2006.

[54] H. Wang, Z. Wu, Y. Liu, and Y. Wang, "Influences of various Pt dopants over surface platinized TiO_2 on the photocatalytic oxidation of nitric oxide," *Chemosphere*, vol. 74, no. 6, pp. 773–778, 2009.